Forest et al., https://doi.org/10.1083/jcb.201705107

JCB

JOURNAL OF CELL BIOLOGY

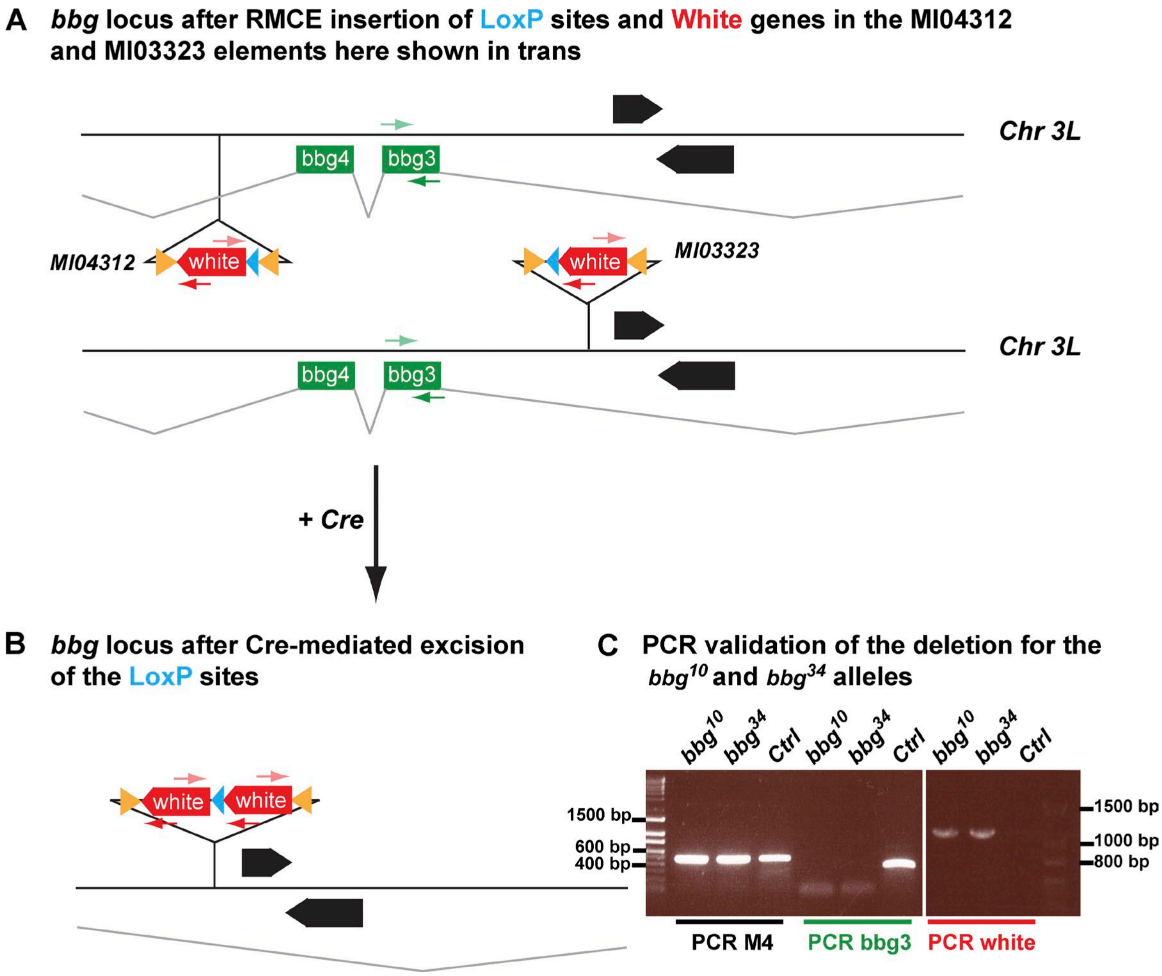

Figure S1. **Generation of new *bbg* alleles by recombinase-mediated cassette exchange. (A)** Schematic representation of the *bbg* locus focusing on the third and fourth exons (bbg3 and bbg4 in green). The two MiMIC insertions flanking these exons have been engineered by recombination-mediated cassette exchange (RMCE) to introduce a w^+ marker and a LoxP site (in blue). Green and red arrows represent specific primer sets used for mapping. **(B)** *bbg* locus after a boost of Cre recombinase. **(C)** PCR validation of these events on adult fly homozygous genomic DNA. PCR M4 is a PCR with primers for the *E(spl)-m4* gene and was unaffected in this procedure. This approach led to specific deletions (shown in this image are the bbg^{10} and bbg^{34} alleles) at high frequency.

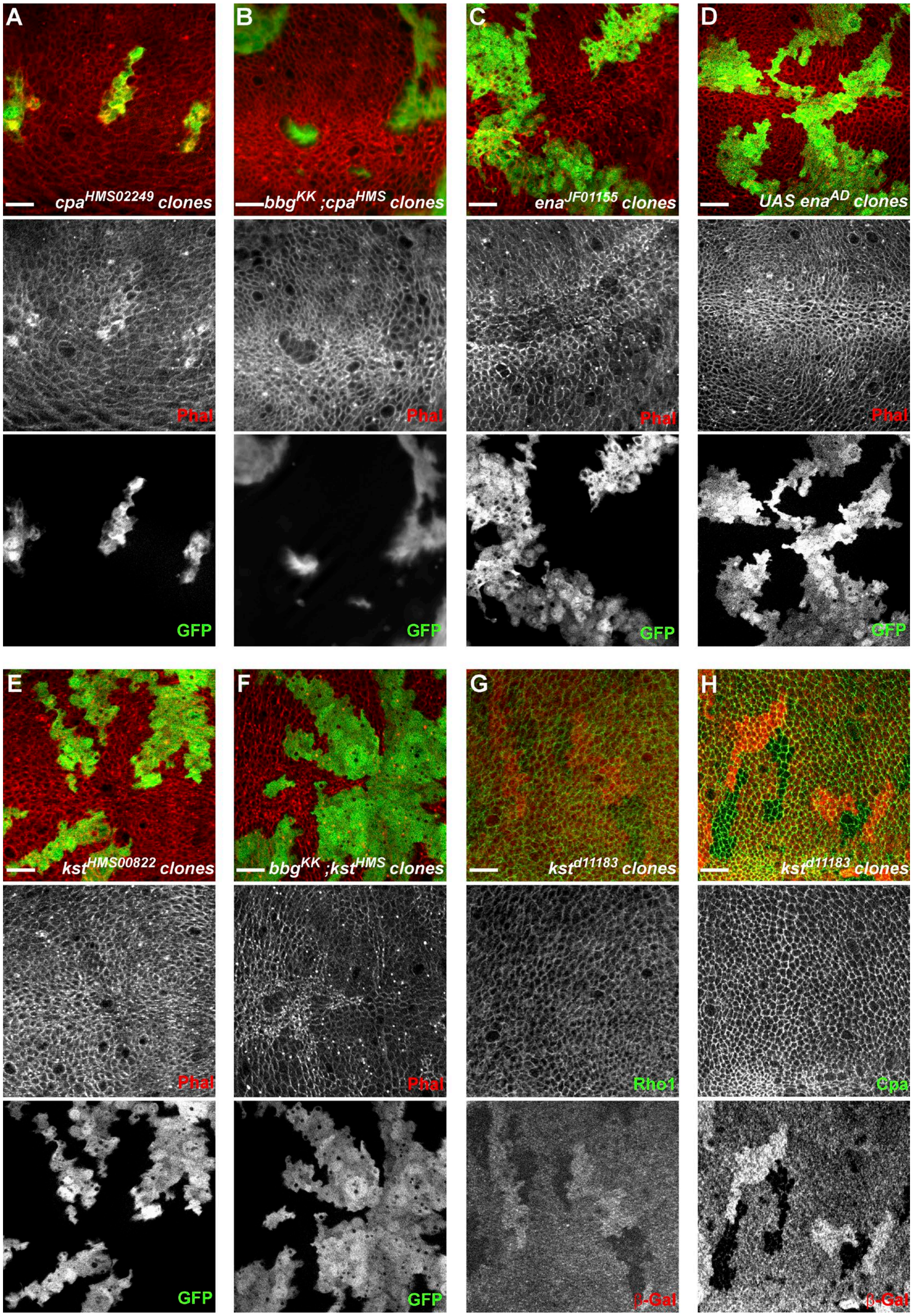

Figure S2. **Cortical F-actin cytoskeleton in *bbg* or *kst* mutants. (A–F)** Overexpression clones marked by GFP (green) leading to depletion of *cpa* (A), double depletion of *cpa* and *bbg* (B), depletion of *ena* (C), overexpression of *ena* (D), depletion of *kst* (E), or double depletion of *bbg* and *kst* (F), and showing the organization of the cortical apical F-actin (red). No changes in F-actin could be observed after *ena* level modulation or *kst* depletion. A strong decrease of apical F-actin was seen only in *bbg*-depleted cells (B and F), imposing even on the *cpa* depletion–induced F-actin enrichment (A). **(G and H)** kst^{d11183} mutant clones in the larval wing disc marked by the absence of β-galactosidase (red) and marked for the actin regulators Rho1 (G, green) and Cpa (H, green). No significant difference was observed between WT and *kst* mutant cells. Bars, 10 µm.

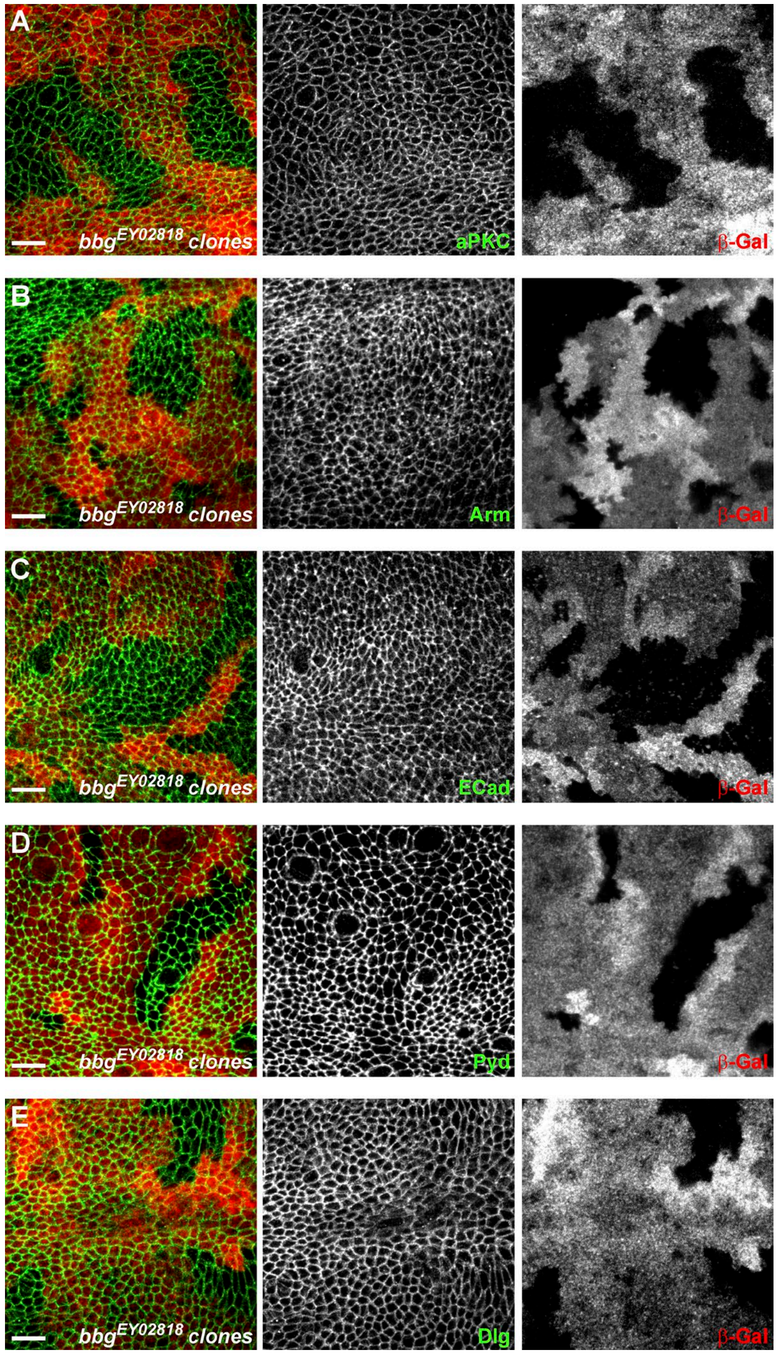

Figure S3. **Epithelial apical–basal polarity is unaffected in *bbg* mutants. (A–E)** *bbg*^{EY02818} mutant clones in the larval wing disc marked by the absence of β-Galactosidase (red) and marked for the apical–basal markers aPKC (A, green), armadillo (B, green), E-Cad (C, green), polychaetoid (D, green), and Dlg (E, green). No significant difference was observed between WT and *bbg* mutant cells. Bars, 10 µm.

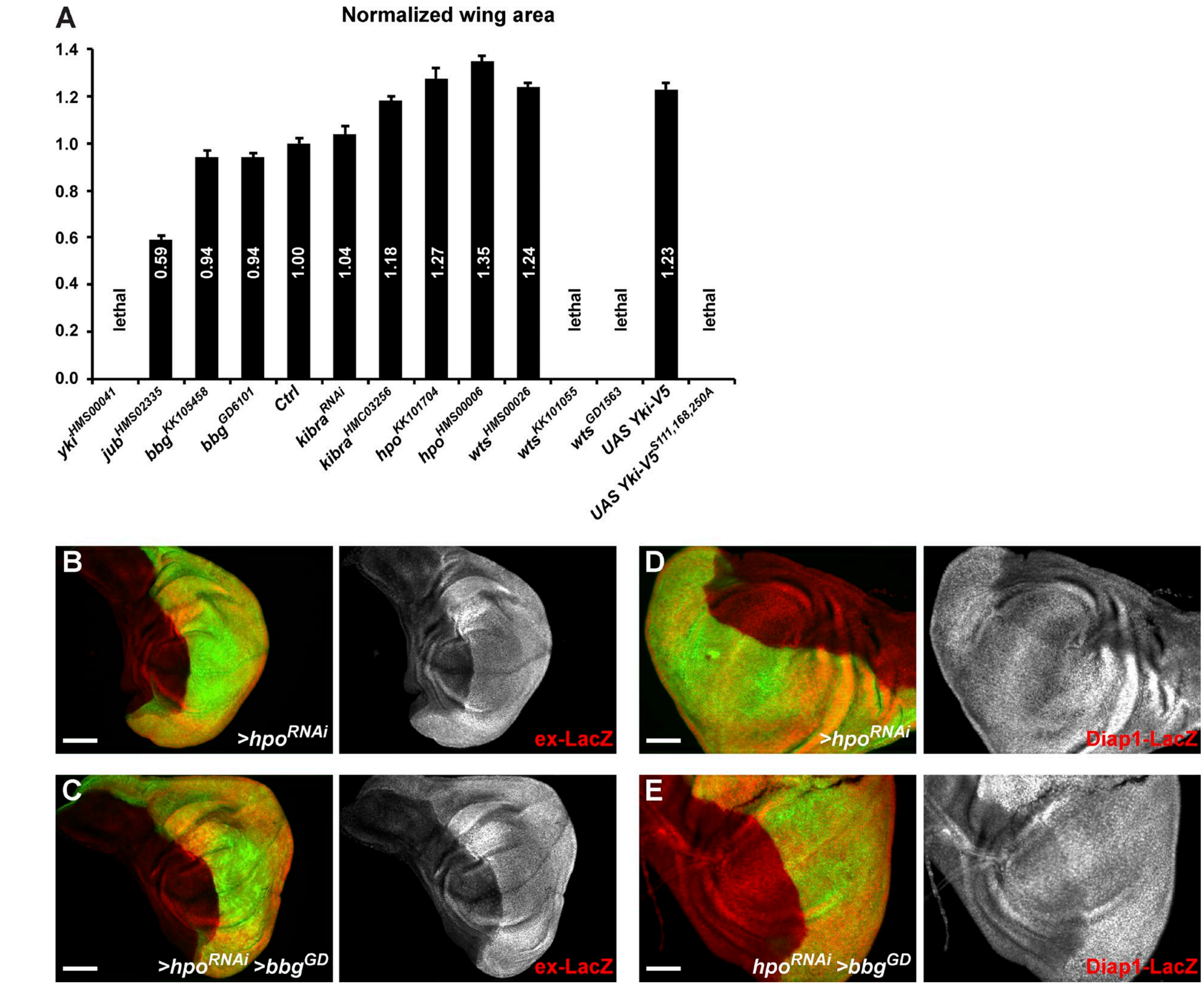

Figure S4. **Bbg and the Hippo pathway. (A)** Adult female *Drosophila* wing size after *nubG4*-driven RNAi knockdown at 25°C of the indicated genotypes. The wing area for each genotype is expressed as a ratio compared with the mean wing area of the *nubG4>UAS GFP* controls (*Ctrl*). SD is shown; *n* = 17–31 independent female wings. Some combinations did not produce any viable adults and are labeled "lethal." **(B–E)** Pouch region of third instar larva wing imaginal discs. Effect of *hh-Gal4*–driven RNAi knockdown in the posterior compartment marked by GFP (green) on the expression of the Yki activity reporters *ex-LacZ* (B and C, red) and *Diap1-LacZ* (D and E, red). The up-regulations of *ex-LacZ* and *Diap1-LacZ* caused by *hpo* knockdown (B and D) were not affected by the further knockdown of *bbg* (C and E). Quantifications are shown in Fig. 5. Bars: (B and C) 100 µm; (D and E) 50 µm.